ChemComm

Accepted Manuscript

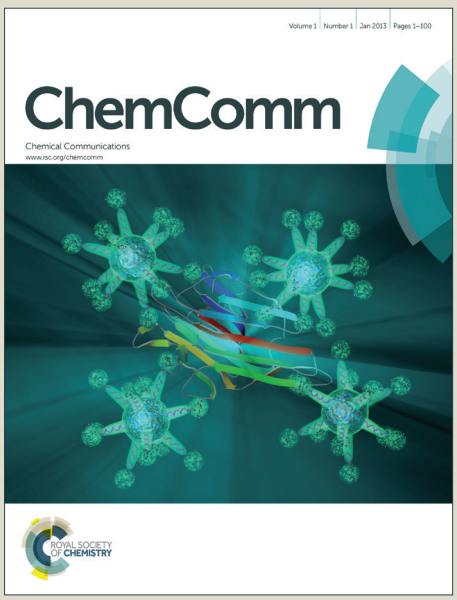

ROYAL SOCIETY OF CHEMISTRY

www.rsc.org/chemcomm

Cite this: DOI: 10.1039/c0xx00000x

www.rsc.org/xxxxxx

ARTICLE TYPE

The Extraordinary Catalytic Ability of Peroxiredoxins: a Combined Experimental and QM/MM Study on the Fast Thiol Oxidation Step

Ari Zeida,[a] Anibal M. Reyes,[b] Mariano C. G. Lebrero,[c] Rafael Radi,[b] Madia Trujillo[b]* and Darío A. Estrin[a]*

Received (in XXX, XXX) Xth XXXXXXXXX 20XX, Accepted Xth XXXXXXXXX 20XX
DOI: 10.1039/b000000x

Peroxiredoxins (Prxs) catalyze the reduction of peroxides, a process of key relevance in a variety of cellular processes. The first step in the catalytic cycle of all Prxs is the oxidation of a cysteine residue to sulfenic acid, which occurs 10^3-10^7 times faster than in free cysteine. We present an experimental kinetics and hybrid QM/MM investigation to explore the reaction of Prxs with H_2O_2 using alkyl hydroperoxide reductase E from *Mycobacterium tuberculosis* as a Prx model. We report for the first time the reaction thermodynamical activation parameters of H_2O_2 reduction by a Prx, which show that the protein lowers significantly the activation enthalpy, with an unfavourable entropic effect, compared to the uncatalyzed reaction. The QM/MM simulations show that the remarkable catalytic effects responsible for the fast H_2O_2 reduction in Prxs are mainly due to an active-site arrangement, which establishes a complex hydrogen bond network activating both reactive species.

Peroxiredoxins (Prxs, EC 1.11.1.15) are ubiquitous broad spectrum peroxidases that catalyze the reduction of peroxides such as hydrogen peroxide (H_2O_2), organic hydroperoxides and peroxynitrite, via the oxidation of a cysteine (Cys) residue, the peroxidatic Cys (Cys_P) which occurs several orders of magnitude faster than in the case of free Cys. Although this reaction has been extensively studied in different Prxs, the molecular basis underlying the catalysis of the peroxide reduction step accomplished by these enzymes, remains poorly understood.

Prxs have been demonstrated to play protective roles against the development of different diseases in which oxidative stress play a pathogenic role.[1-3] They have high expression levels (up to 1% of cellular proteins)[4] and very fast catalytic rates in the order of ~10^5-10^8 $M^{-1}s^{-1}$.[5,6] Competitive kinetics analysis predicts that Prxs are responsible for the reduction of most of mitochondrial and cytoplasmic H_2O_2 in eukaryotic cells.[4,7] Besides their role in antioxidant defences, some Prxs have been identified as key participants in the regulation of redox signalling pathways.[8-10] The catalytic cycle of Prxs involves the two-electron oxidation of Cys_P, the formation of a disulfide bond with a second Cys residue or low molecular weight thiol, and the posterior recycling step through thiol/disulfide exchange reactions.[11] Prxs can be classified into six subfamilies by sequence analysis (AhpC-Prx1, Prx6, Prx5, Tpx, BCP-PrxQ, AhpE; http://csb.wfu.edu/prex.test/prxInfo.php, see reference 12 for a detailed description); or in three classes by a mechanistic criteria based on the requirement of a second resolving Cys.[10] Importantly, the active site of Prxs is highly conserved, and they all share a common first step of the catalytic cycle in which the thiolate in Cys_P is oxidized to sulfenic acid:

$$CyS^- + ROOH \rightarrow CySOH + RO^- \text{ (eq. 1)}$$

This is a rapid and chemically interesting event, which consists in a bimolecular nucleophilic substitution on the reactive oxygen atom of the peroxide. The key issue in the molecular basis of the catalytic ability of peroxiredoxins is to understand how the active site microenvironment of these enzymes can accelerate by factors of ~10^3-10^7 H_2O_2 reduction compared to the uncatalyzed reaction, i.e. that of free Cys in aqueous solution. Fast reactivity was firstly attributed to the low Cys_P pK_a, assuring thiolate availability at physiological pH values, mostly due to a pair of very conserved charge-stabilizers arginine (Arg) and threonine (Thr) residues in the active-site. However, this phenomenon can only account for a ten- fold acceleration of H_2O_2 reduction velocity rates at pH 7.4.[13] Very recently, by means of a thorough structural analysis of members of different subfamilies of Prxs, a complete overview of the active-site structure and its interactions with the peroxide substrate has been accomplished.[14] Moreover, the authors proposed a transition state (*ts*) model, in which a complex hydrogen bond network is assumed to be responsible for *ts* stabilization. Summing up, the above presented evidence point out to the fact that all Prxs are expected to behave according to the same general oxidative mechanism.

In this work we performed a thorough investigation of the key oxidation reaction mechanism of Prxs using *Mycobacterium tuberculosis* AhpE (*Mt*AhpE) as a model. *Mt*AhpE is the representative of AhpE, a novel subgroup of the Prxs family. It is a 1-Cys Prx and it is mostly an A-type dimer in solution.[15] Structural analysis shows the resemblance, not only at the sequence level but from a structural viewpoint, of this Prx active-site with other proteins of the family.[15] We have previously conducted a complete kinetic characterization,[16,17] finding that *Mt*AhpE reduces H_2O_2 with a rate constant equal to 8.2 x 10^4 $M^{-1}s^{-1}$ at pH 7.4 and 25ºC. The reason of our choice is that *Mt*AhpE shows changes in intrinsic fluorescence intensity that occur during protein oxidation facilitating single-turnover kinetic determinations which are not possible in most other cases, and for which indirect approaches are required.[18] Moreover, H_2O_2

reduction by this enzyme is much faster than by free Cys, but still, it is not so fast as to preclude very precise kinetic experiments using stopped-flow methodologies. This fact allows us to report for the first time activation thermodynamic parameters determinations for Prxs. In addition, we also used a theoretical approach in order to identify and characterize the molecular basis that explains the catalytic ability of these enzymes. Specifically, we compute the free energy profile for the reaction by means of state of the art quantum mechanics (at DFT-*PBE* level)/molecular mechanics (QM/MM)[19] umbrella sampling simulations (see Supplementary Information). This simulation scheme, which has been previously applied with success in

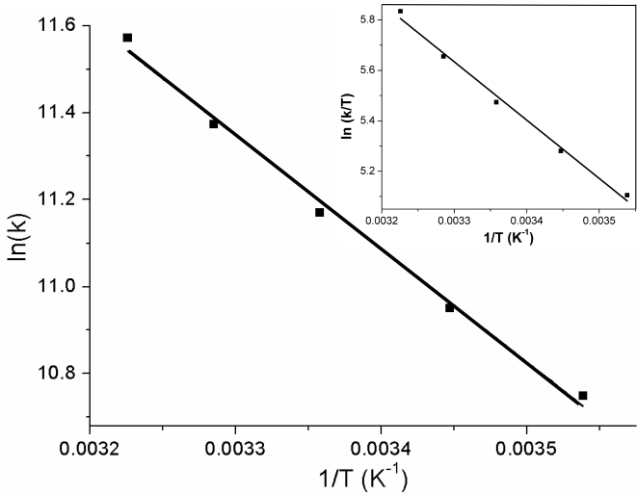

Figure 1 Rate constant temperature dependence of the reduction of H_2O_2 by *Mt*AhpE at pH 7.4. Arrhenius and Eyring's analysis (inset) of rate constants determined at T=10, 16.5, 25, 31.5 and 37°C are shown. Figure corresponds to one independent experiment that was repeated three times with almost identical results.

similar processes,[20,21] allows us to compute free energies profiles as well as the evolution of the electronic properties along the reaction coordinate, within a realistic representation of the enzyme microenvironment.

Rate constant temperature-dependence of the reduction of H_2O_2 by *Mt*AhpE at pH 7.4 is presented in Figure 1 (to observe k_{obs} (s^{-1}) as a function of H_2O_2 concentration, see supplementary Figure S1). As described previously,[16] the enzyme catalyzes the reaction by a factor of ~6 x 10^4 in terms of apparent rate constants at pH 7.4, and ~5 x 10^3 in terms of pH-independent rate constants, compared to the reaction with free Cys at 25°C.[22] Remarkably, the analysis of the thermodynamic activation parameters compared to those obtained for free Cys[22] (Table 1), illustrates that the $\Delta G^{\#}$ decrease is explained by means of two opposing terms; while this Prx is capable to greatly diminish $\Delta H^{\#}$, which is almost four times smaller in the enzyme than in solution, the unfavourable entropic contribution ($-T\Delta S^{\#}$=5.7±0.7 kcal mol^{-1}), signifies that the $-T\Delta S^{\#}$ term represents more than 50% of the total $\Delta G^{\#}$ at 25°C. This may indicate that Prxs active site are designed to significantly improve the interaction with the reaction's *ts*, shaping a very ordered *ts* (as will be described below), resulting in a net decrease of $\Delta G^{\#}$.

Previous to the exploration of the reaction's free energy profile, a survey of the structure and dynamical behaviour of the *Mt*AhpE dimer was performed by means of classical molecular dynamics simulations (MD), with the crystal structure of the reduced enzyme as starting point (PDBid: 1XXU)[15] and considering the unprotonated form of Cys_P (Cys_{45}), since its pK_a has been reported as 5.2.[16] As general to all Prxs, Cys_P is positioned at the N-terminal helix α2 at the bottom of the active-site pocket and its thiolate negative charge is mainly stabilized by conserved Thr and Arg residues (Thr_{42} and Arg_{116} in *Mt*AhpE). Particularly, the Arg_{116} is strongly positioned towards Cys_P via the interaction with other two residues: the mostly conserved Glu_{48} and the backbone of Pro_{135}.

Table 1 Kinetic and thermodynamics activation parameters for the reduction of H_2O_2 by free Cys and *Mt*AhpE. Standard deviations in parenthesis when available.

	k_2 ($M^{-1}s^{-1}$)[a]	E_{act} (kcal mol^{-1})	$\Delta H^{\#}$(kcal mol^{-1})	$\Delta S^{\#}$(cal K^{-1} mol^{-1})	$\Delta G^{\#}$ (kcal mol^{-1})
free Cys[b]	14.9	17.0	16.4(0.3)	1.7(1.1)	15.9
*Mt*AhpE-Cys_{45}	8.2 x 10^4 (1.5)	5.7(0.7)	4.8(0.5)	-19.1(1.9)	10.5

[a] k_{app} were measured at 25° and pH 7.4[16] or at different pHs,[22] and real, pH-independent k_2 were calculated using the equation

$$k_{app} = k_2\left(\frac{10^{-pK_a^{Cys}}}{10^{-pK_a^{Cys}}+10^{-pH}}\right)$$

[b] data taken from reference 22

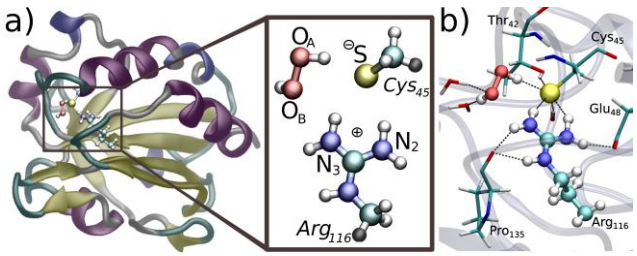

Figure 2 a) Representation of the *Mt*AhpE (only one monomer is shown) with H_2O_2 in the active-site (*rs*), along with a schematic view of the quantum subsystem, i.e. Cys_{45} and Arg_{116} sidechains and the H_2O_2 moiety. Atoms names as referred in the text, and colored according to their type: white, hydrogen; cyan, carbon; red, oxygen; blue, nitrogen; yellow, sulfur. Link atoms are shown in grey. b) Representative structure of the *rs*. H_2O_2, S atom from Cys_{45} and Arg_{116} sidechain are represented as balls, while sidechains of Thr_{42}, Glu_{48} and Pro_{135} and water molecules are represented by sticks.

Although Cys_P lies at the base of the active site pocket, the thiolate moiety exhibits significant solvation, as it is not a hydrophobic active-site. Moreover, in the presence of H_2O_2 in the Michaelis complex (reactant state, *rs*), 2-3 water molecules are also present, but the thiolate group becomes less solvated (see supplementary information Figure S2). The *rs* is characterized by a strong H-bond type interaction between S and O_A, with an ($S-O_A-O_B$) angle of ~90° (See Figure 2 and supplementary information Table S1). Besides the interaction between the sulfur atom of Cys_P and H_2O_2, the peroxide moiety is located in this particular position inside the active-site, due to two weak H-bonds with the amide-N atom of Cys_P and with N_3 of Arg_{116}. A comparision of this Michaelis complex with the one obtained by X-ray crystallography in the archeal Prx *Ap*TPx (the only experimental determined structure of a Prx with H_2O_2 in its active-site)[23] shows some subtle differences; although the peroxide is maintained by very similar interactions in both cases,

*Ap*TPx-H_2O_2 complex presents a slightly longer S-O_A distance and a quasi-linear S-O_A-O_B angle.

Umbrella sampling QM/MM simulations were started from the classically modelled *rs* (see Figure 2), and the reaction was considered as a substitution displacement, choosing as reaction coordinate the difference between the O_A-O_B and the S-O_A distances. The obtained free energy profile is depicted in Figure 3. The reaction is clearly exergonic, with a change in the free reaction energy of about -38 kcal mol^{-1}, also in agreement with previously reported information for the uncatalyzed reaction.[20] Even though it shows a $\Delta G^{\#}$ of ~14 kcal mol^{-1}, resulting in a modest overestimation in comparison with the experimental determined one (see Table 1), it represent a ~4 kcal mol^{-1} decrease compared to our previous study of a model thiolate in aqueous solution,[20] which is consistent with the experimental determined $\Delta\Delta G^{\#}$=5.4 kcal mol^{-1} and with the ~5000 fold increase in reactivity observed.

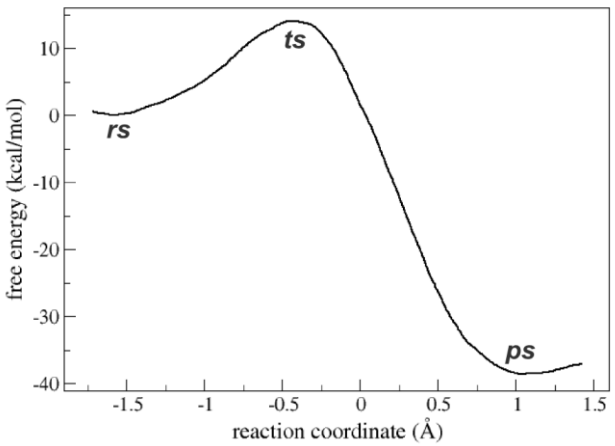

Figure 3 Free energy profile of the reduction of H_2O_2 by *Mt*AhpE obtained by QM/MM umbrella sampling. The reaction coordinate was defined as the difference between the O_A-O_B distance and the S-O_A distance, and was sampled from -1.7 to 1.4 Å.

This simulation scheme allows getting a microscopic insight into the reaction mechanism, as well as a detailed description of the system properties at different stages of the process (see the 3D animation available in supporting information for illustration). As proposed by Hall and co-workers,[14] the reaction consists, at least at first stages, of a simple bimolecular S_N2 substitution, with S as the nucleophile and O_A as the electrophile. The set of molecular factors that determines catalysis can be integrated within the *ts* stabilization framework,[24] so a detailed description of *ts* behaviour is of great significance. Firstly, as expected for this kind of substitutions, the *ts* is almost "linear" with a (S-O_A-O_B) angle of ~160°, where the peroxidatic bond is practically broken and the S-O_A bond is in formation process (see Figure 4 and supplementary information Table S1). This approach and alignment of the peroxide's oxygen atoms towards the thiolate, is guided by a great improvement in the interactions between H_2O_2 and the enzyme that were described for the *rs*. O_A is markedly positioned by a strong H-bond with the amide-N atom of Cys_P and leaded by the interaction with Arg_{116}. This Arg_{116} along with Thr_{42}, retain the S atom in the reactive position. O_B points outside the pocket and interacts with water molecules. Indeed, the active-site residues present a complex H-bond intra- and inter-molecular network (Figure 4). In this context, Nagy *et al* reported that the above mentioned Arg residue plays a key role in activating the peroxide that also involves hydrogen bonding to a second Arg conserved in some Prx families (Prx1, Prx6 and AhpE).[25] However, the role of the latter is under debate.[14,26] Our simulations indicate that if there is a role of this second Arg it is indirect by assisting in the building of the active-site architecture. The strong interactions with Arg_{116} and Thr_{42} residues are the main responsible for the *ts* stabilization and the concomitantly significant reduction in the $\Delta H^{\#}$, which in turn results in a decrease in $\Delta G^{\#}$ in spite of the unfavourable entropic contribution.

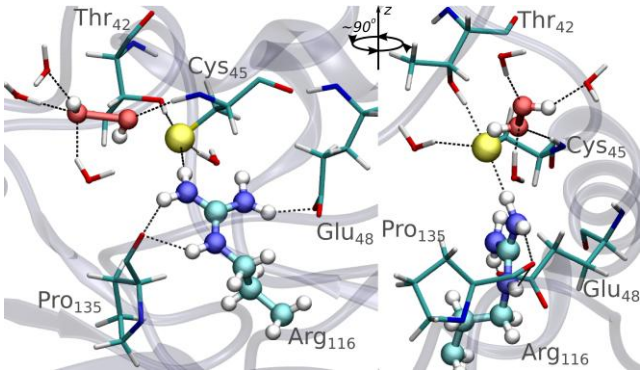

Figure 4 Two different views of a typical snapshot corresponding to the *ts*. H_2O_2, S atom from Cys_{45} and Arg_{116} sidechain are represented as balls, while sidechains of Thr_{42}, Glu_{48} and Pro_{135} and water molecules are represented by sticks. Atoms are coloured according to their type: white, hydrogen; cyan, carbon; red, oxygen; blue, nitrogen; yellow, sulfur. Important hydrogen bonds are indicated by dashed black lines.

As previously described,[20] the reaction is driven by the tendency of the slightly charged peroxide's oxygen atom to become even more negative, therefore the system must experience a significant charge redistribution (see Mulliken's population over relevant atoms upon reaction in supplementary information Figure S4). At the same time as the S atom looses negative charge, its charge is been acquired by both O_A and O_B atoms. The set of interactions described above, guides this process, allowing charge redistribution to take place at a lower energy cost compared to the reaction in aqueous solution. Specifically, our results confirm the key role of Arg_{116}. In the reactant state both N_2 and N_3 Arg atoms stabilize the thiolate moiety of the reactive Cys. In the transition state, the incipient negative charge on sulfenic O_A atom is partially stabilized by Arg_{116} N_3 that then establishes a strong interaction in the product state (Table S1). This shows that the plasticity of Arg_{116} motions is probably the key issue in the catalysis.

After the system has reached the *ts*, a proton transfer from O_A to O_B occurs, as previously reported for low molecular weight model thiolate oxidation by H_2O_2 (see supplementary information Table S1).[20,27] Therefore, the reaction yields the oxidized Cys_P in the unprotonated form of sulfenic acid (Cys_PSO^-) and a water molecule. The product state (*ps*) is characterized by important changes in the active-site microenvironment, Arg_{116} moves inside the pocket in order to maintain the contacts with both S and O_A atom, the newly oxidized Cys_PSO^- side chain loses its interaction with Thr_{42} and the negative charge concentrated in O_A atom is now stabilized by Arg_{116} (so much that a proton can be

considered as "shared" by this two moieties), the strong interaction with the amide-N atom and water molecules that fill the pocket (see supplementary information Table S1 and Figure S3).

In summary, our calculations support the idea of a bimolecular nucleophilic substitution S_N2 type mechanism, with an internal proton transfer. No evidence of acid-base catalysis was observed. Thus, the extraordinary catalytic ability of these enzymes towards peroxide reduction is not related with a change in the overall mechanism in comparison with the same reaction in aqueous solution. The power of Prxs lies on their capability to stabilize the *ts* over *rs* due to an active-site design, which is capable to lay out a complex H-bond network activating both reactive species, i.e. Cys_P and the peroxide substrate. The activation parameters experimentally determined are in agreement with this kind of *ts* stabilization.

The precise knowledge of the catalytic mechanisms of Prxs provides the basis to understand their prominent roles in antioxidant defenses and redox signaling pathways.[1-3] Moreover, the interactions between specific amino acids and the peroxide substrate at the *rs* and *ts* described herein will be helpful for the design of potential inhibitors of these enzymes.[28] This could provide tools for the treatment of infectious diseases as well as specific forms of cancer where peroxides play a cytotoxic role,[29] or to modulate particular signaling processes.[30] However, the design of inhibitors for specific Prxs will be challenging, due to the very conserved peroxidatic active site structure in the different members of the family.

Notes and references

[a] *Departamento de Química Inorgánica, Analítica y Química-Física and INQUIMAE-CONICET, Facultad de Ciencias Exactas y Naturales, Universidad de Buenos Aires, Ciudad Universitaria, Pab. 2, C1428EHA Buenos Aires, Argentina E-mail: dario@qi.fcen.uba.ar*

[b] *Departamento de Bioquímica and Center for Free Radical and Biomedical Research, Facultad de Medicina, Universidad de la República, Av. Gral Flores 2125, CP 11800, Montevideo, Uruguay E-mail: madiat@fmed.edu.uy*

[c] *IQUIFIB-Dpto. Química Biológica, Facultad de Farmacia y Bioquímica, Universidad de Buenos Aires, Buenos Aires, Argentina*

† Electronic Supplementary Information (ESI) available: Experimental procedures, computer simulations details, additional results and 3D animation specifications included in the supporting information. See DOI: 10.1039/b000000x/

‡ Acknowledgment: This work was partially supported by the Universidad de Buenos Aires, CONICET, Centro de Biología Estructural Mercosur (CeBEM). MT and RR acknowledge the financial support of the Agencia Nacional de Investigación e Innovación (FCE_2011_1_5706, ANII, Uruguay) and Comisión Sectorial de Investigación Científica (CSIC), Universidad de la República and National Institutes of Health (R01 AI095173), respectively.

1 K. F. Bell, G. E. Hardingham, *Antioxid. Redox Signalling.* 2011, **14**, 1467.
2 T. Eismann, N. Huber, T. Shin, S. Kuboki, E. Galloway, M. Wyder, M. J. Edwards, K. D. Greis, H. G. Shertzer, A. B. Fisher, A. B. Lentsch, *Am. J. Physiol. Gastrointest. Liver Physiol.* 2009, **296**, 266.
3 X. Hu, Z. Weng, C. T. Chu, L. Zhang, G. Cao, Y. Gao, A. Signore, J. Zhu, T. Hastings, J. T. Greenamyre, *J. Chen. Neurosci.* 2011, **31**, 247.
4 C. C. Winterbourn, *Nat. Chem. Biol.* 2008, **4**, 278.
5 L. B. Poole in *Peroxiredoxin Systems*, (Eds.: L. Flohé, J. R. Harris). Springer, New York, 2007, pp. 61.
6 M. Trujillo, G. Ferrer-Sueta, L. Thomson, L. Flohe, R. Radi, *Subcell. Biochem.* 2007, **44**, 83.
7 A. Cox, C. C. Winterbourn, M. Hampton, *Biochem. J.* 2010, **425**, 313.
8 L. M. Randall, G. Ferrer-Sueta, A. Denicola, *Method. Enzymol.* 2012, **527**, 41.
9 L. Flohé, *Method. Enzymol.* 2010, **473**, 1.
10 Z. A. Wood, L. B. Poole, P. A. Karplus, *Science* 2003, **300**, 650.
11 A. Hall, K. Nelson, L. B. Poole, P. A. Karplus. *Antioxid. Redox Signalling*. 2011, **15**, 795.
12 L. Soito, C. Williamson, S. T. Knutson, J. S. Fetrow, L. B. Poole, K. J. Nelson, *Nucleic Acids Res.* 2011, **39**, D332.
13 G. Ferrer-Sueta, B. Manta, H. Botti, R. Radi, M. Trujillo, A. Denicola, *Chem. Res. Toxicol.* 2011, **24**, 434.
14 A. Hall. D. Parsonage, L. B. Poole, P. A. Karplus, *J. Mol. Biol.* 2010, **402**, 194.
15 S. Li, N. A. Peterson, M. Y. Kim, C. Y. Kim, L. W. Hung, M. Yu, T. Lekin, B. W. Segelke, J. S. Lott, E. N. Baker, *J. Mol. Biol.* 2005, **346**, 1035.
16 M. Hugo, L. Turell, B. Manta, H. Botti, G. Monteiro, L.E. Netto, B. Alvarez, R. Radi, M. Trujillo, *Biochemistry* 2009, **48**, 9416.
17 A. M. Reyes, M. Hugo, A. Trostchansky, L. Capece, R. Radi, M. Trujillo, *Free Rad. Biol. Med.* 2011, **51**, 464.
18 R. Ogusucu, D. Rettori, D. C. Munhoz, L. E. Netto, O. Augusto, *Free Rad. Biol. Med.* 2007, **42**, 326–334.
19 H. M. Senn, W. Thiel, *Angew. Chem.* 2009, **121**, 1220
20 A. Zeida, R. Babbush, M. C. González Lebrero, M. Trujillo, R. Radi, D. A. Estrin, *Chem. Res. Toxicol.* 2012, **25**, 741.
21 A. Zeida, M. C. González Lebrero, R. Radi, M. Trujillo, D. A. Estrin, *Arch. Biochem. Biophys.* 2013, **539**, 81.
22 D. Luo, S. W. Smith, B. D. Anderson, *J. Pharm. Sci.* 2005, **94**, 304.
23 T. Nakamura, Y. Kado, T. Yamaguchi, H. Matsumura, K. Ishikawa, T. Inoue, *J. Biochem-Tokio*, 2010, **147**, 109.
24 M. Garcia-Viloca, J. Gao, M. Karplus, D. G. Truhlar, *Science* 2004, **303**, 186.
25 P. Nagy, A. Karton, A. Betz, A. V. Peskin, P. Pace, R. J. O'Reilly, M. B. Hampton, L. Radom, C. C. Winterbourn, *J. Biol. Chem.* 2011, **286**, 18048.
26 C. A. Tairum Jr, M. A. de Oliveira, B. B. Horta, F. J. Zara, L. E. Netto, *J. Mol. Biol.* 2012, **424**, 28.
27 B. Cardey, M. A. Enescu, *ChemPhysChem* 2005, **6**, 1175.
28 A. Lodola, M. De Vivo, *Adv. Protein Chem. Struct. Biol.* 2012, **87**, 337.
29 W. Lu, Z. Fu, H. Wang, J. Feng, J. Wei, J. Guo. *Mol. Cell. Biochem.* 2014, **387**, 261.
30 H. A. Woo, H. Z. Chae, S. C. Hwang, K. S. Yang, S. W. Kang, K. Kim, S. G. Rhee. *Science* 2003, **300**, 653.